Journal of the Palaeontological Society of India
Volume 67(1), June 30, 2022: 126-138

ISSN 0552-9360

An assessment of foraminiferal species distribution and stable-isotope anomalies at a methane-hydrate mound in the Gulf of Mexico

Paul Aharon[1*], Emil Platon[2] & Barun K. Sen Gupta[3]

JPSI

Using a manned submersible, a 25-cm-long sediment core was acquired at upper bathyal depth in the Gulf of Mexico from a mound underlain by methane hydrates at the threshold of stability. The main objective of the core investigation was to elucidate little-understood effects of gas-hydrate dissociation on benthic foraminiferal ecology, stratigraphy, and stable isotopes.

Our results show that intense methane seepage has decimated, but not obliterated, the benthic foraminiferal community that includes many facultative anaerobes, dominated by two species of *Bolivina.* The remnant community has continued to exist at this site for over 2000 years. A shift from a much higher foraminiferal density to persistent low values is observed in the lowermost part of the core. A major oil spill in the Gulf of Mexico in 2010 caused similar devastation to the foraminiferal community, and drastically reduced the density.

Planktonic (*Globigerinoides ruber*) and benthic foraminiferal tests (*Bolivina ordinaria* and *Bolivina albatrossi*) yield $\delta^{13}C$ and $\delta^{18}O$ profiles that are inversely correlated and exhibit anomalously negative carbon and positive oxygen isotope values up to maxima of -10.2‰ and 3.9‰ (VPDB), respectively. The isotope anomalies are attributed to anaerobic oxidation of ^{13}C-depleted biogenic methane and intake of ^{18}O-rich fluids released during hydrate dissociation. Two sequential sulfate-methane transition zones (SMTZs), with sedimentation rates of 8.2 and 27.5 cm Ka^{-1}, are coeval with two distinct intervals in the *G. ruber* isotope profiles. Three lines of evidence attest to the complexity of reconstructing methane flow from foraminiferal records. (i) Both planktonic and benthic foraminiferal tests serve as templates for secondary carbonate overgrowths. (ii) Decoupling of the overgrowths from the primary biogenic calcite tests is intractable, and therefore stable isotopes cannot be used as a tool to confirm whether *Bolivina* may live and thrive in anoxic sediments.

Keywords: Gas hydrates, oxygen and carbon isotopes, radiocarbon dating, Benthic foraminifera, carbonate overgrowths

ARTICLE HISTORY

Manuscript received: 05/02/2022
Manuscript accepted: 08/04/2022

*[1]Department of Geological Sciences, University of Alabama, Box 870338, Tuscaloosa, AL 35487, USA; [2]7470 s 3500 E Salt Lake City, UT 84121, USA; [3]Department of Geology & Geophysics, Louisiana State University, Baton Rouge, La 70803, USA. *Corresponding author's e-mail: paharon@ua.edu*

INTRODUCTION

Calcareous benthic foraminifera have long attracted scientific attention, because of their great value as clues to geochronology and paleoenvironments. Apart from features of community composition (varying abundances of species), the carbon and oxygen isotopes in their tests has proved exceptionally useful in palaeoceanographic reconstructions (e.g., Rohling and Cooke, 1999; Gooday, 2003; 2019).

The advent of ocean drilling programs and availability of research submersibles led to an extensive exploration of marine-based gas hydrates that store a vast amount of the "greenhouse" methane gas on the continental margins (Kvenvolden, 1995). The atmospheric methane potency on global warming is well known (Wuebbles and Hayhoe, 2002), but the factors controlling the stability of gas hydrates, and the exact methane pathway from the seafloor to the atmosphere, are poorly understood (Hesse, 2002; 2003; Brewer, 2006; Ruppel *et al.,* 2022).

The quest to find a marker of past methane emissions singled out benthic foraminifera on account of observed ^{13}C-variability in tests of living foraminifera that mirror pore-fluid chemistry alterations (McCorkle *et al.,* 1990). Apparent tolerance of some benthic foraminiferal species to oxygen-free environments (Sen Gupta and Aharon, 1994; Sen Gupta *et al.,*1997; Panieri *et al.,* 2009; Orsi *et al.,* 2020) and carbon-isotope negative excursions in tests from different stratigraphic levels have offered support to a proposed link between large methane outgassing and global warming events (Wefer et al. 1994; Dickens *et al.,* 1995; Kennett *et al.,* 2000; Maslin *et al.,* 2004; Panieri *et al.,* 2014; Joshi *et al.,* 2014). However, investigations of benthic foraminifera at active gas hydrate settings have unraveled alteration of the isotope compositions of the benthic primary biogenic tests thus questioning the veracity of the paleo-gas hydrate studies (Stott *et al.,* 2002; Torres *et al.,* 2003; Rathburn *et al.,* 2003;

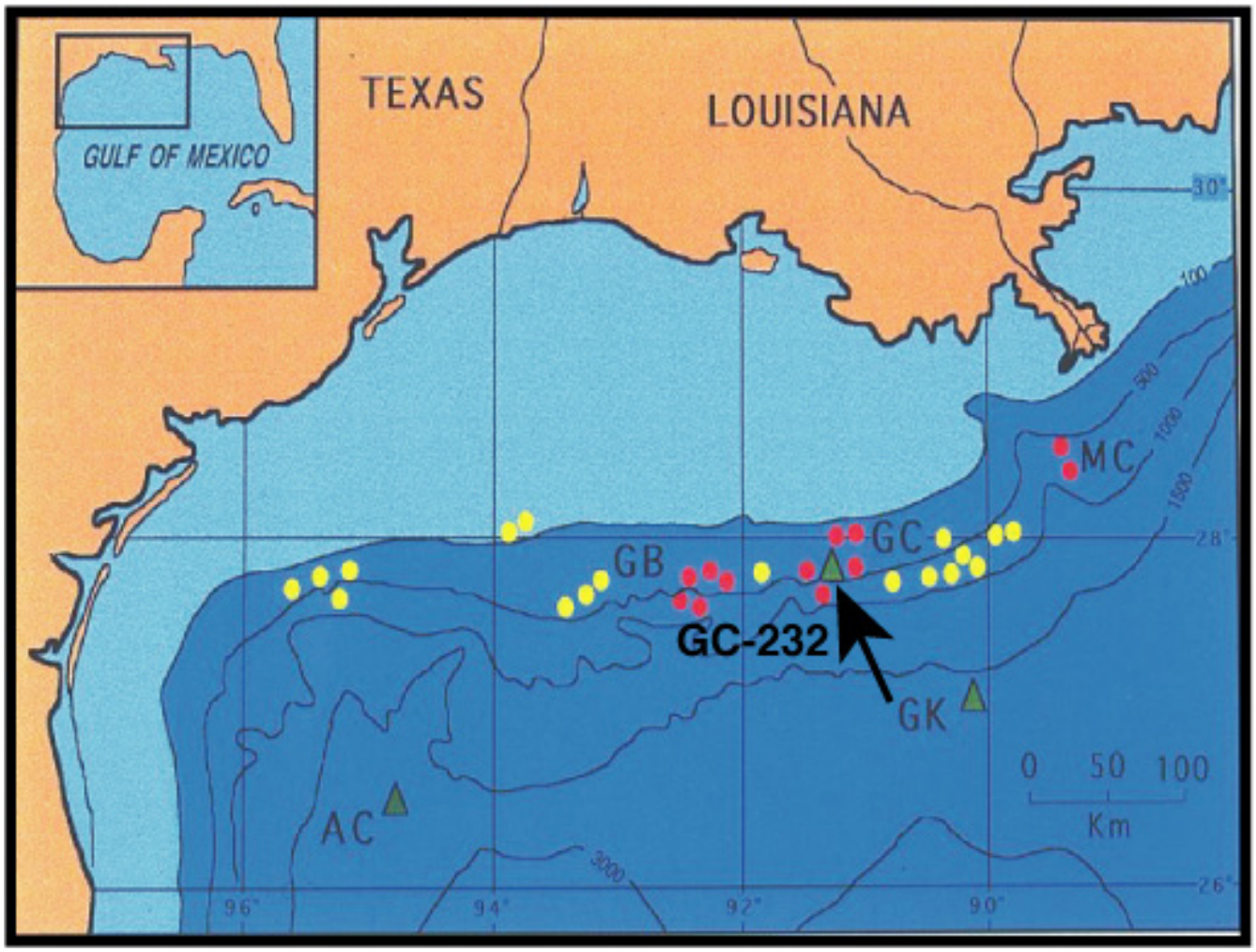

Fig. 1. Location map of the lease-block GC-232, Green Canyon, Gulf of Mexico. Yellow and red dots represent sites of seafloor sediments investigated during multiple manned submersible dives.

Cannariato and Stott, 2004; Herguera *et al.,* 2014; Panieri et al, 2017).

In this study, we present two aspects of an investigation of a hydrate-bearing sediment mound in the Gulf of Mexico: (1) ecology and stratigraphy of the foraminiferal assemblage, and (2) carbon and oxygen isotope geochemistry of co-existing planktonic and endobenthic foraminifera. Assessment of the isotope records in conjunction with pore fluids chemistry alterations allows identification of the microbial processes occurring in the sediment and their control on post-depositional alterations of foraminiferal tests. Our results have an important bearing on the dependability of foraminiferal archives as recorders of methane fluxes through the sediment.

STUDY SETTING

We took multiple push cores and box cores in the upper bathyal Green Canyon (lease-block GC-232), northern Gulf of Mexico, using the manned submersible *Johnson Sea-Link II*. Within this area, the coordinates of our main target, a 25-cm-long push core (JSL-2900-PC2), studied for both geochemistry and faunal record, were 24° 44.64' N and 91°19.05' W; at a depth 567 m (Fig. 1). The rugged, hummocky, seafloor here contains meter-high mounds cladded by soft mud sediment. The mounds overlie a shallow salt diapir whose upward movements give rise to growth faults breaching the seafloor and serving as conduits for slow-seeping hydrocarbons to the seafloor (Fig. 2). White, solid gas-hydrate patches outcrop on the margin of the steeper slopes or near the crest of mounds. These patches go through cycles of formation and dissolution, causing growth, exposure, sublimation, and deflation of the mounds (MacDonald *et al.,* 2003).

The hydrate mound studied here is covered by patches of white and orange *Beggiatoa* spp. mats and rich communities of thiotrophic tube-worms and methanotrophic/ thiotrophic bathymodiolid mussels (Fig. 3 a). The cores for this particular study were acquired with the submersible's arm through a patch of white *Beggiatoa* mat on the flank of the mound (Fig. 3 b).

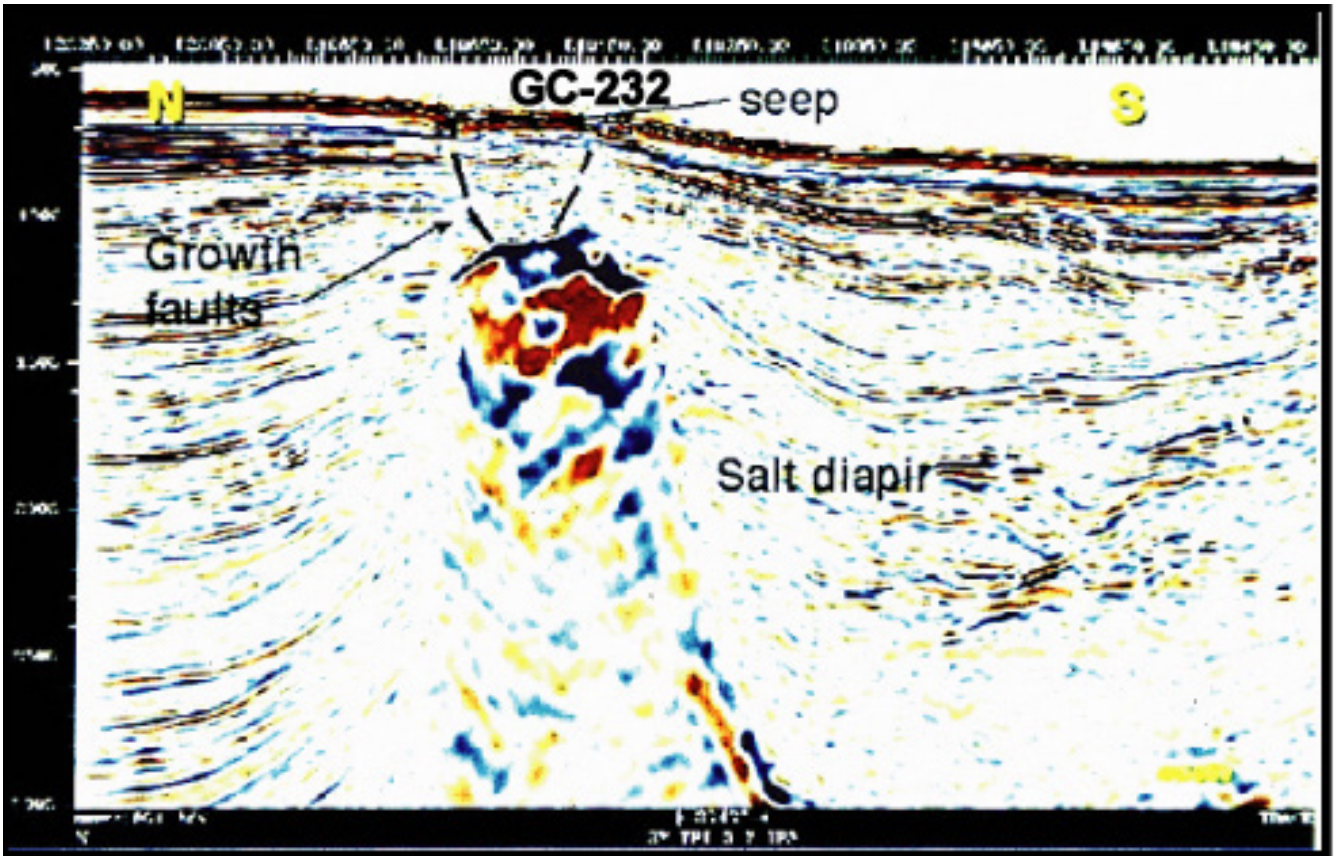

Fig. 2. 3-D seismic profile trending N-S, highlighting the shallow salt dome underlying GC-232, and growth faults intersecting the seafloor and serving as conduits for fluids and hydrocarbon seepage. Horizontal and vertical scales are 7 and 2 km, respectively. Note the acoustic wipeout zone underlying the GC-232 seafloor area.

SEDIMENTOLOGY AND PORE-FLUID GEOCHEMISTRY

The primary objective of the acquisition of multiple cores on the GC-232 hydrate mound (Fig. 3) was to combine the studies of sedimentology and pore fluids geochemistry (Fu, 1998; Hackworth, 2005; Bordoloi, 2007) with the study of foraminiferal ecology, community structure, biostratigraphy, and isotope geochemistry (Platon, 2001) in order to discern the processes occurring in sediments underlain by gas hydrates at their threshold of stability (Fig. 4).

The sediment in core JSL-2900-PC2 is overlain by a white *Beggiatoa* mat and consists of intensely black-colored, fine hemipelagic mud containing large (> 1 cm) to fine (< 1mm) carbonate nodules, whole gastropod shells, shell fragments and foraminiferal tests (Fig. 5 a). Biodegraded crude pods and oil stains are most abundant in the lower section of the core (Fig. 5 a).

Geochemical assays attest to the anoxic nature of the sediment and unravel the alteration of the seawater-derived pore fluids by microbial processes fueled by methane. The sulfidic nature of the pore fluids is revealed by the paired sulfate-sulfide concentrations in cores taken next to JSL-2900-PC2 (Fig. 3 b), exhibiting a pronounced anti-correlation between the two phases (Fig. 5 b). The fading of the seawater-derived sulfate within the upper 25 cm of the sediment and its replacement by reduced sulfide mark the sulfate-methane transition zone (SMTZ). Upward migration of methane and downward diffusion of sulfate at the SMTZ prompt coupled microbial sulfate reduction-methane oxidation processes under anaerobic conditions (Aharon, 2000; Aharon and Fu, 2000; 2003; Panieri *et al.,* 2017). Freshening of the pore fluids, co-occurring with an anomalous ^{18}O-enrichment of up to 1.5‰ (VSMOW) (Fig. 5 c), is attributed to the dissociation of the underlying gas hydrates, because (i) gas hydrate traps fresh water in the lattice that is released during dissociation (Hesse and Harrison, 1981; Hesse, 2003), and (ii) gas hydrates are enriched in ^{18}O relative to seawater by 2.8‰ to 3.2‰ (Maekawa and Imai, 2006).

METHODS

Ecology and biostratigraphy

We used subsamples from two push cores (PC) and one box core (BSc) for the census of living foraminifera. Separately, we collected biostratigraphic data (0-24 cm) from push core JSL-2900-PC2 that also provided samples for the isotope study. All these coring sites were located within a few meters of each other. After retrieval, the top 1 cm sediment

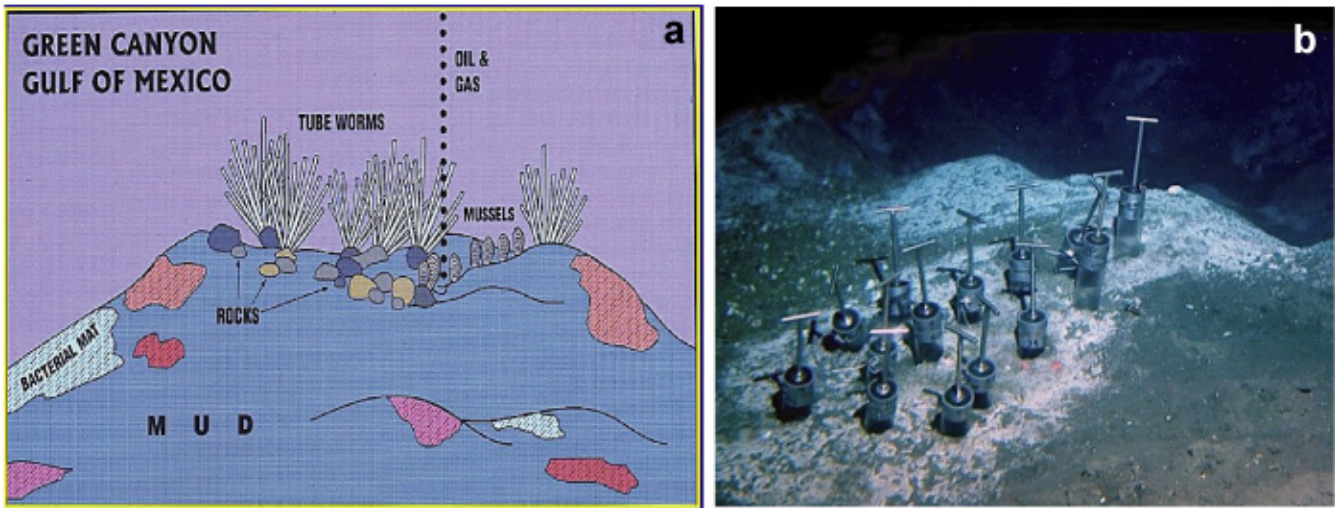

Fig. 3. Hydrate mound on GC-232 at about 560 m water depth, cored during JSL dive #2900. (a) Cartoon illustrating the surface of the mound covered by fine hemipelagic mud with thiotrophic tube worms, methanotrophic/thiotrophic bathymodiolid mussels, white and orange-colored *Beggiatoa spp.* mats and carbonate rocks. Note the oil droplets and gas bubbles streaming from the mound into the surrounding seawater. (b) Photograph showing acquisition of multiple sediment cores with the submersible robot arm from a white *Beggiatoa spp.* mat, including cores JSL-2900-PC2 and 97-2900-WM discussed in the text.

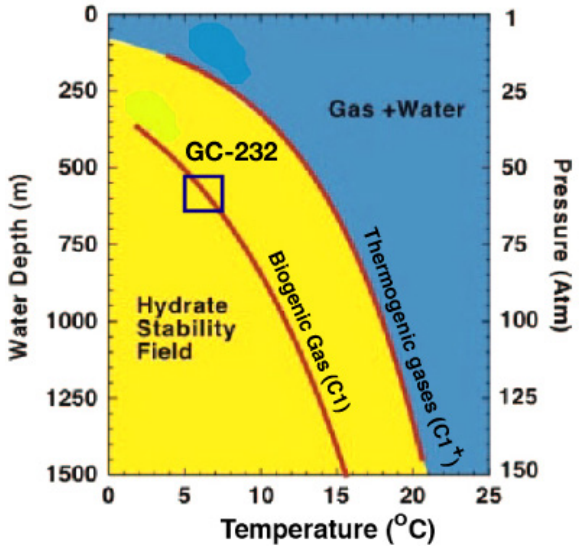

Fig. 4. Gas-hydrate stability field as a function of pressure and ambient water temperature (modified from Hesse, 2003). At a pressure of 56 atm and 7.4 °C the biogenic methane-hydrate underlying the mound on GC-232 will be unstable. However, under the same conditions a hydrate consisting of thermogenic mixture of gases ($C1^+$) will be well within the stable field.

was removed from every core, stained with Rose Bengal, and saved in plastic jars. The rest of the material was kept frozen until it was processed in the laboratory. Specimens >63 µm were used for foraminiferal counts.

Geochemistry

The methods used onboard to squeeze pore fluids from the designated GC-232 cored sediments, the specific description of the sediments and their subsequent geochemical analyses have been detailed by Aharon (2000) and Aharon and Fu (2000; 2003) and will not be repeated here. Below we outline the laboratory methods employed to perform oxygen and carbon isotope analysis of foraminiferal tests.

The sediment extracted from the core lining was cut into 1cm thick slices and dried at room temperature. Tests of a planktonic species (*Globigerinoides ruber*) and two endobenthic species (*Bolivina albatrossi* and *Bolivina ordinaria*) were handpicked under a binocular microscope from 1 cm-thick slices of the sediment core. The two *Bolivina* species were selected for the isotope analysis because of (i) their relative abundance throughout the core, and (ii) the presence of their living individuals (stained by Rose Bengal) in the top 2-3 cm of sediment cores taken at other seep sites in Green Canyon (Sen Gupta *et al.,* 1997). Additionally, tests of co-existing *G. ruber* and *Bolivina* spp. were acquired from sediment cores taken at approximately the same water depth in hemipelagic muds from isobathyal, hydrate-free sites, to serve as control for the foraminiferal tests in the hydrate mound. Relative paucity of the two *Bolivina* species in a few sampling intervals required mixing in proportion representing their distribution in seep-free sediment samples.

Tests were repeatedly cleaned of adhering debris in an ultrasonic bath filled with distilled water, and dried in an oven at 50°C. Samples of about ten *G. ruber* and up to thirty *Bolivina* tests were reacted under vacuum with 100% orthophosphoric acid in a mini-extraction online with a Nier-type automated triple-collector 6/60 mass spectrometer. The difference in the number of individual tests per sample is because of the planktonic calcite tests being much larger and heavier than the paired benthic species. Liberated CO_2 was cryogenically separated from other gases and introduced into the mass spectrometer for oxygen and carbon isotope measurements. The results are reported in the conventional "δ" notation in permil (‰) relative to the VPDB standard. The precision and reproducibility of the isotope measurements (chemistry and mass spectrometry combined) are estimated to be ±0.1‰ on the basis of standard repeats. The isotopic variability attributed to each sample is estimated to be

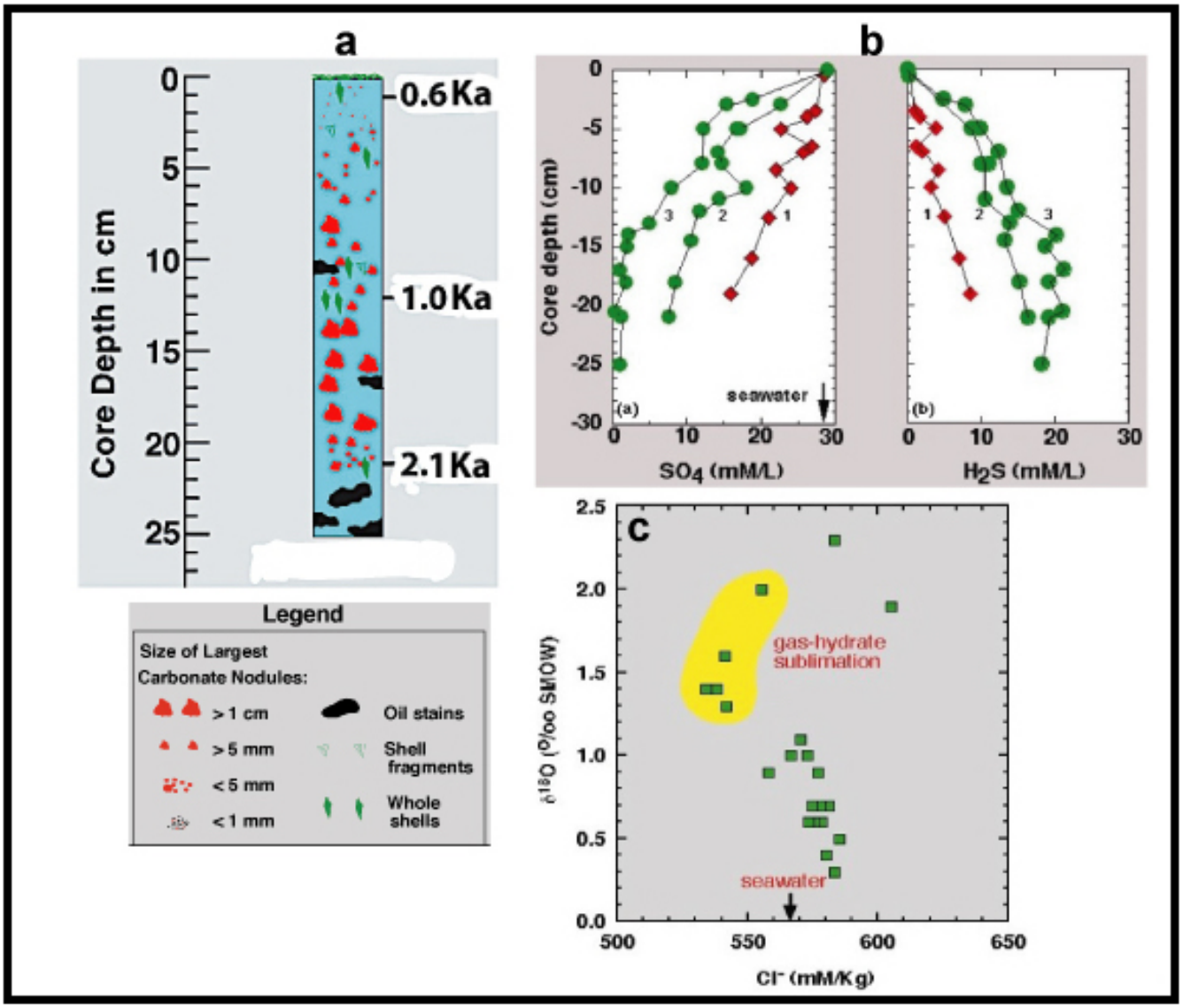

Fig. 5. Representative sedimentology and selected aspects of pore fluid geochemistry of the hydrate mound in GC-232 (Hackworth and Aharon, 1998; Hackworth and Aharon, 2000; Aharon and Fu, 2000; Aharon and Hackworth, 2001; Hackworth, 2005). (a) Cartoon exhibiting sedimentary components in the core. Radiocarbon dates were acquired from a twin core (97-2900-WM) identical to JSL-2900-PC2 (see text). (b) Sulfate and sulfide concentrations in sediments from GC-232 mound (). Note the inverse correlation between the two sulfur compounds. Maximum anaerobic oxidation of methane (AOM) by a coupling of sulfate-reducing bacteria and methanotrophic archaea occurs at the sulfate-methane transition zone (SMTZ) where upward migrating methane and downward migrating of sulfate meet. Maximum precipitation of authigenic carbonates occurs at the depth of the SMTZ (see text). (c) $\delta^{18}O$ and chloride concentrations in pore fluids exhibit ^{18}O-enrichment and chloride dilution caused by methane-hydrate dissociation. Hydrates are heavier in $\delta^{18}O$ by 2.8 to 3.2‰ relative to seawater (Maekawa and Imai, 2006) and their lattice contains freshwater that causes chloride dilution.

±0.26‰ for $\delta^{18}O$ and ±0.25‰ for $\delta^{13}C$ on the basis of variance analysis of 59 replicates (Aharon, 2003).

Three radiocarbon determinations were acquired from the vagrant deep-sea gastropod genus *Gymnobela* (Warren and Bouchet, 1993), whose dead shells were buried in the mound sediment (Fig. 5 a). These cleaned, acid-etched shells, ~0.5 cm in size, were recovered from three separate layers in core 97-2900-WM (twin to our principal core JSL-2900-PC2), and were dated by radiocarbon at the National Ocean Sciences Accelerator Mass Spectrometry (NOSAMS). The measured dates were corrected for a reservoir effect of 800 years, specific to the Gulf of Mexico upper bathyal depth (Aharon *et al.,* 1997), but not converted to calendar ages for reasons explained below. The sedimentation rates were calculated from the difference in core depths divided by the difference in radiocarbon dates (SR = $\Delta z/\Delta t$) (Fig. 5 a). The sedimentation rates in the upper half and in the lower half of the core are thus 27.5 cm Ka^{-1} and 8.2 cm Ka^{-1}, respectively, the former being higher by a factor of three compared to typical upper bathyal sedimentation rate of 9 ±2 $cmKa^{-1}$ in seep-free sites from the Gulf of Mexico (Santschi and Rowe, 2008).

Although we took the necessary precautions to remove all the potential contaminants from the gastropod shells, the possibility of some remnant methane-derived carbonate infill cannot be ignored. That is because any methane-derived carbonate contaminant will dilute the "true" $\Delta^{14}C$ value with a $\Delta^{14}C=0$, causing the radiocarbon dates to be

"older" than "true" values. Although radiocarbon dates in correct stratigraphic order (Fig. 5 a) argue against any substantial offset caused by contaminants, the possibility of an offset toward older dates must be acknowledged. Our view is to consider the radiocarbon dates as "maximum" dates, meaning that in the absence of any methane-derived carbonate contaminants the dates can only be younger, but not older, than the ones we are reporting here. The calculated sedimentation rates in the core are not impacted because their derivation is based on difference in dates and not on their absolute values.

RESULTS

Living foraminifera

At the dive location of JSL 2900, two push cores (PC) and a box core (Bsc) were taken to investigate the vertical distribution of living foraminifera. Box core Bsc EP9 was retrieved from an orange *Beggiatoa* mat and PC EP11 from a white *Beggiatoa* mat. PC EP10 was taken from a spot where no bacterial mat was visible, but carbonate nodules and oil droplets in the core indicated the site to be within the area of hydrocarbon seepage.

The maximum number of living foraminifera (i.e., Rose-Bengal-stained tests) was found in the top 1-cm samples of the 3 cores (mean = 19.33 individuals in 30 cc of sediment). Common species in this surface layer were *Bolivina albatrossi*, *B. ordinaria*, *Paracassidulina neocarinata*, *Fursenkoina compressa* and *Trifarina bradyi*. Below the 1-cm level, the assemblage density drops rapidly in Bsc EP9 and PC EP11; in PC EP10, there were no living individuals at deeper levels (Fig. 6).

Sequential changes in species distribution

We identified 73 species from the 24 stratigraphic subsamples of JSL2900-PC2 (Table 1). However, for many rare species, the specific epithet could not be determined, and the binomen is left incomplete. Most of the fully named species are illustrated in Platon (2001) and are also shown in Lobegeier and Sen Gupta (2008) and Sen Gupta et al. (2009).

The maximum number of species in a sample (none living below the top 5 cm) was 46, and was found in the lowermost sample studied (24 cm below the top, Fig. 7). Decreasing trends of species richness were recorded within the 22-20 cm, 16-13 cm, and 12-9 cm intervals. The Shannon Wiener Index (Figure 7) decreases in the 24-19 cm and 17-9 cm intervals, but increases in the 19-17 and 9-0 cm intervals. Equitability trends (Figure 8) are more noticeable, average values being 0.45 for the 24-21 cm interval, 0.63 for the 20-15 cm interval and 0.74 in the younger part of the core.

The foraminiferal density (number of tests in one gram of dry sediment) shows a clear upward decrease in the bottom section of the core, from 24 to 19 cm. In samples from this part, the density may be >2000, whereas in the upper section (from 19 cm to the top), the values never reach 500, and

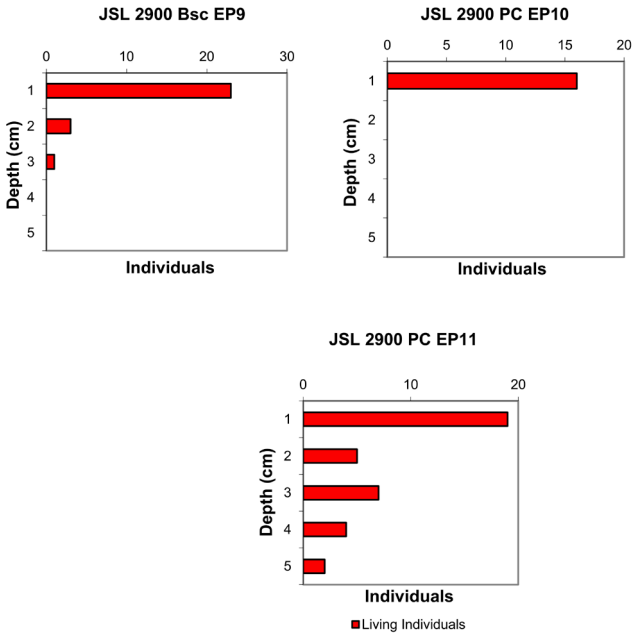

Fig. 6. Downcore variations in living foraminiferal density (number of individuals in 30 cc of sediment) in three cores from Green Canyon (Bsc = box subcore; PC = push core).

are <100 in most samples. Within these limits, however, the density rises at the sediment-water interface (0-1 cm sample), where the pore fluid is largely seawater. There is no evidence that post-mortem dissolution of foraminiferal tests by the corrosive interstitial fluid has been more severe in the younger, depauperate part of the core (19 to 0 cm), than in the older part. Thus, we judge the much-reduced

Table 1. Benthic foraminifera present in core JSL-2900-PC2.

SPECIES	*Hyalinonetrion* sp. cf. *H. gracillimum* (Seguenza)
Amphicoryna hirsuta (d'Orbigny)	*Karreriella bradyi* (Cushman)
Anomalinoides io (Cushman)	*Lagena* sp.
Bolivina albatrossi Cushman	*Lagenammina difflugiformis* (Brady)
Bolivina barbata Phleger & Parker	*Laticarinina pauperata* (Parker & Jones)
Bolivina daggarius Parker	*Lenticulina* sp. 1
Bolivina fragilis Phleger & Parker	*Lenticulina* sp. 2
Bolivina lowmani Phleger & Parker	*Lenticulina* sp. 3
Bolivina ordinaria Phleger & Parker	*Lenticulina* sp. 4
Bolivina subaenariensis Cushman	*Marginulina* sp. 1
Bolivina sp.	*Marginulina* sp. 2
Bulimina aculeata d'Orbigny	*Miliolinella circularis* (Bornemann)
Bulimina alazanensis Cushman	*Neolenticulina variabilis* (Reuss)
Bulimina marginata d'Orbigny	*Nonion* sp.
Bulimina striata d'Orbigny	*Oolina* sp.
Bulimina sp.	*Osangulariella rugosus* (Phleger & Parker)
Cassidulina curvata Phleger & Parker	*Paracassidulina neocarinata* (Thalmann)
Cassidulina laevigata d'Orbigny	*Planulina ariminensis* d'Orbigny
Cassidulina sp. 1	*Planulina foveolata* (Brady)
Cassidulina sp.2	*Polymorphina* sp.
Cibicides pachyderma (Rzehak)	*Pseudononion* sp.
Cibicidoides incrassatus (Fichtel & Moll)	*Pullenia bulloides* (d'Orbigny)
Cibicidoides sp.	*P. subsphaerica* Parr
Epistominella exigua (Brady)	*Pyrgo murrhina* (Schwager)
Epistominella sp.	*Quinqueloculina* sp. 1
Eponides regularis Phleger & Parker	*Quinqueloculina* sp. 2
Fissurina laevigata Reuss	*Quinqueloculina* sp. 3
Fissurina. sp. 1	*Quinqueloculina* sp. 4
Fissurina sp. 2	*Sigmoilina* sp.
Fissurina. sp. 3	*Siphonina bradyana* Cushman
Fissurina. sp. 4	*Stainforthia complanata* (Egger)
Fissurina sp. 5	*Stetsonia minuta* (Parker)
Gavelinopsis translucens Phleger & Parker	*Trifarina bradyi* Cushman
Globobulimina sp.	*Triloculina* sp. 1
Globocassidulina subglobosa Brady	*Triloculina* sp. 2
Hansenisca soldanii (d'Orbigny)	*Uvigerina peregrina* Cushman
Hoeglundina elegans (d'Orbigny)	*Valvulineria mexicana* Parker

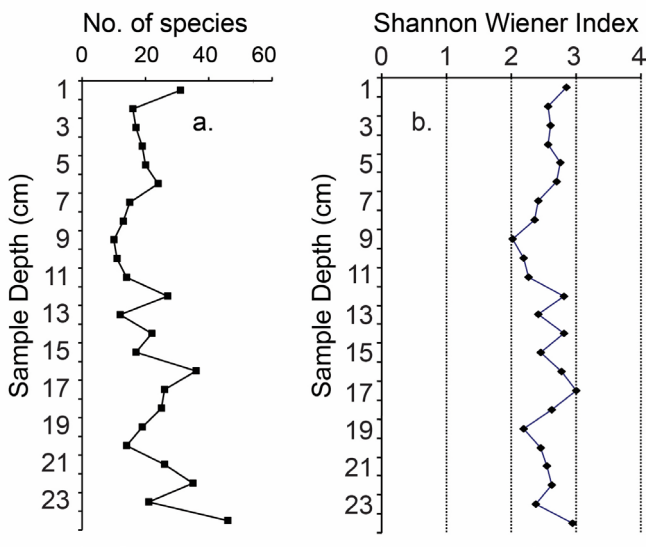

Fig. 7. Species diversity distribution in core JSL-2900-PC2: (a) species richness; (b) Shannon Wiener Index.

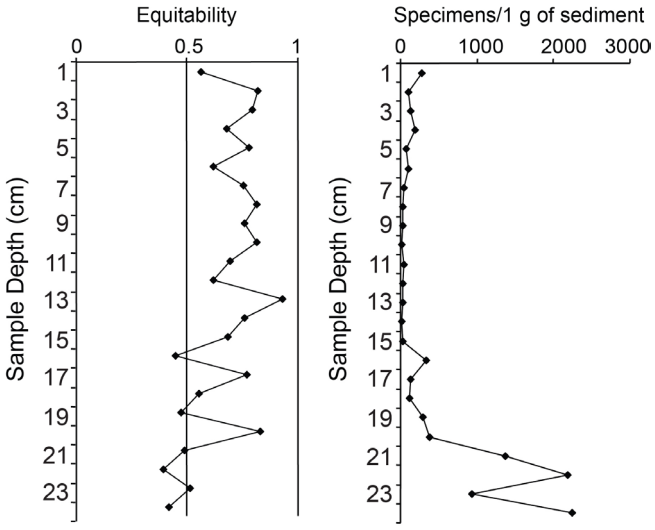

Fig. 8. Stratigraphic distribution of (a) equitability and (b) assemblage density (number of foraminiferal tests in 1gm of dry sediment) in core JSL-2900-PC2.

foraminiferal density above the 19-cm datum to indicate a much-depleted, remnant community. The combination of the decreased number of species and low population densities in the upper section of the core would result in a more uniform distribution of species within the foraminiferal assemblage (Fig. 8). Therefore, increasing trends of equitability in this particular data set are due to the lower numbers of specimens and species in the upper core samples.

Species frequently occurring throughout the core are *Bolivina albatrossi, B. ordinaria, Bulimina aculeta, B. alazanensis, Epistominella exigua, Gavelinopsis translucens, Osangularia rugosa, Paracssidulina neocarinata, Siphonina bradyana, Trifarina bradyi,* and *Uvigerina peregrina.* As determined by Rose Bengal staining, all these species were found alive at other hydrocarbon seep sites in the northern Gulf of Mexico (Sen Gupta *et al.,* 1997; Platon, 2001). Figure 9 shows the stratigraphic distribution of three main genera: *Bolivina (B. albatrossi, B.fragilis, B. lowmani, B. ordinaria), Bulimina* (*B. aculeata, B. alazanensis, B. marginata, B. striata), and Gavelinopsis* (*G. translucens*). Each genus constitutes 10% or more of the assemblage in one or more samples. *Bolivina,* reaching a relative abundance of >25% in a majority of samples, is clearly the dominant genus; the mean abundance of its commonest species (*B. ordinaria*) in JSL2900-PC2 is ~15%.

The results of a Principal Component Analysis further clarify the stratigraphic pattern of foraminiferal distribution in the core. Together, three principal components explain 60.3% of the variance in the data set. High loadings onto factor 1 (accounting for ~22% of the variance) are those of the species *Bolivina albatrossi., Bulimina aculeata, Osangularielloides rugosus,* and *Siphonina bradyana.* Factor 2 (~19% of variance) is strongly loaded by *Bolivina ordinaria, Bulimina alazanensis,* and *Trifarina bradyi*. Factor 3 (~18% of variance) is loaded by *Paracassidulina neocarinata, Planulina ariminensis, P. foveolata,* and *Uvigerina peregrina* (Platon, 2001).

A change in the stratigraphic distribution of factor 1 scores takes place between 13 and 14 cm below the sediment-

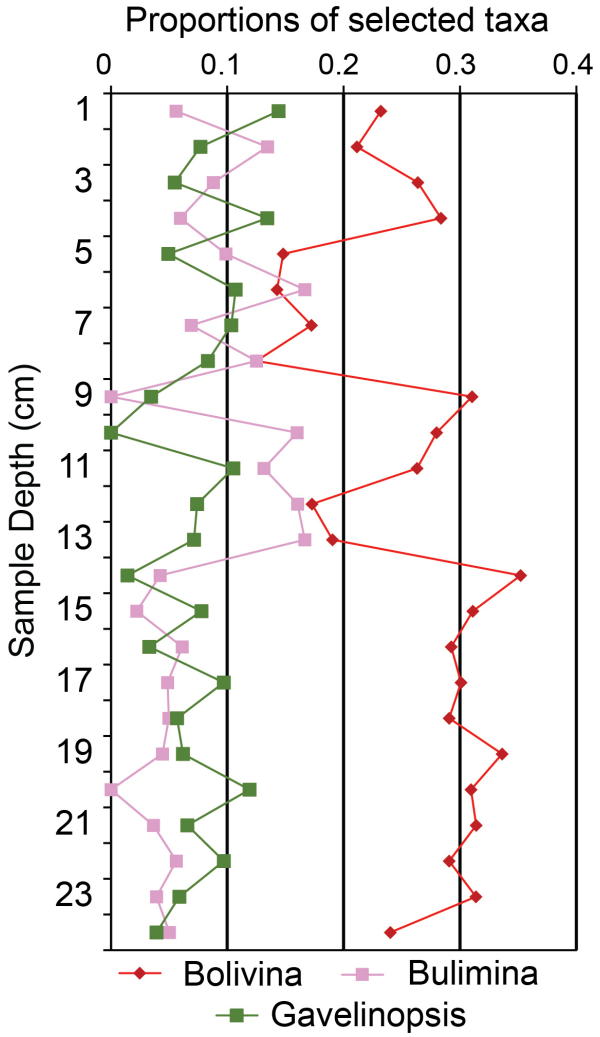

Fig. 9. Relative abundances of three foraminiferal genera in core JSL-2900-PC2.

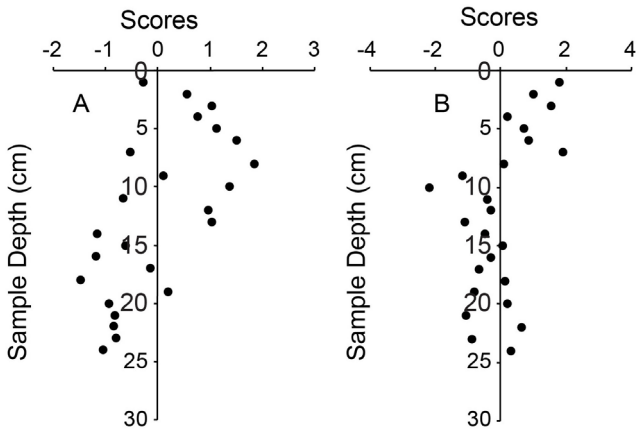

Fig. 10. Stratigraphic plots of foraminiferal factor scores, core JSL-2900-PC2: (A) factor 1; (B) factor 2.

water interface (Fig. 10 A); the mean score for the 24-14 cm interval is -0.80, whereas above the 14 cm level, the mean is 0.68. In the upper part of the core, in the 10-7 cm interval, factor 2 scores steadily decrease from -2.17 to 1.89 (Fig. 10 B). Such large-scale patterns are not decipherable for factors 3 and 4 (Platon, 2001).

Stable isotopes

Carbon and oxygen isotope values of paired planktonic (*Globigerinoides ruber*) and benthic (*Bolivina albatrossi* and *B. ordinaria*) species, and abundance of foraminifera-free total carbonate are listed in Table 2 and graphed against core depth in Figure 11. The $\delta^{13}C$ and $\delta^{18}O$ records of the *G. ruber* tests (Table 2 and Fig. 11 a) match the isotope values of the control samples at the core bottom (0.8 ±0.6‰ and -1.5 ±0.5‰, n=5). The profiles exhibit an upcore trend of anomalously negative ($\delta^{13}C$ = -6.9‰ and $\delta^{18}O$ = -0.1‰) and positive ($\delta^{13}C$ = -0.1‰ and $\delta^{18}O$ = 1.4‰) excursions, respectively, and are inversely correlated. As with *G. ruber*, *Bolivina* $\delta^{13}C$ and $\delta^{18}O$ records (Table 2 and Fig. 11 b) are inversely correlated, and exhibit core-bottom isotope values that match the field of modern species from control sites (-1.5 ±0.4‰ and 2.2 ±0.5‰, n=5). A rapid upward trend is capped at 19 cm depth, with *Bolivina* reaching maximum $\delta^{13}C$ negative and $\delta^{18}O$ positive values of -10.2‰ and 3.9 ‰, respectively. A declining trend accompanied by minor oscillations ends the profiles at the core top.

Dissimilarities between the planktonic and benthic isotope records consist of (i) much greater isotope variability in the former, exhibiting five distinct upcore excursions amounting to several permil in comparison with the relative smoother profiles of the latter, and (ii) greater upcore ^{13}C and ^{18}O depletions and enrichments, respectively, in the benthic record relative to the planktonic record (Figs. 11 a and 11 b). Additionally, the maximum isotope changes in the *Bolivina* profiles occur over the 10-20 cm core depth interval (Fig. 11 b) that coincides with the two "humps" of $CaCO_3$ abundance (Fig. 11 c). The latter is rising from a ~28% abundance at the core bottom, to maximum values of 65% and 70% over the mid-core interval and a subsequent decline to ~32% at the core top (Fig. 6 c). The two "humps" represent peaks of authigenic carbonate deposition expected to occur at the depth

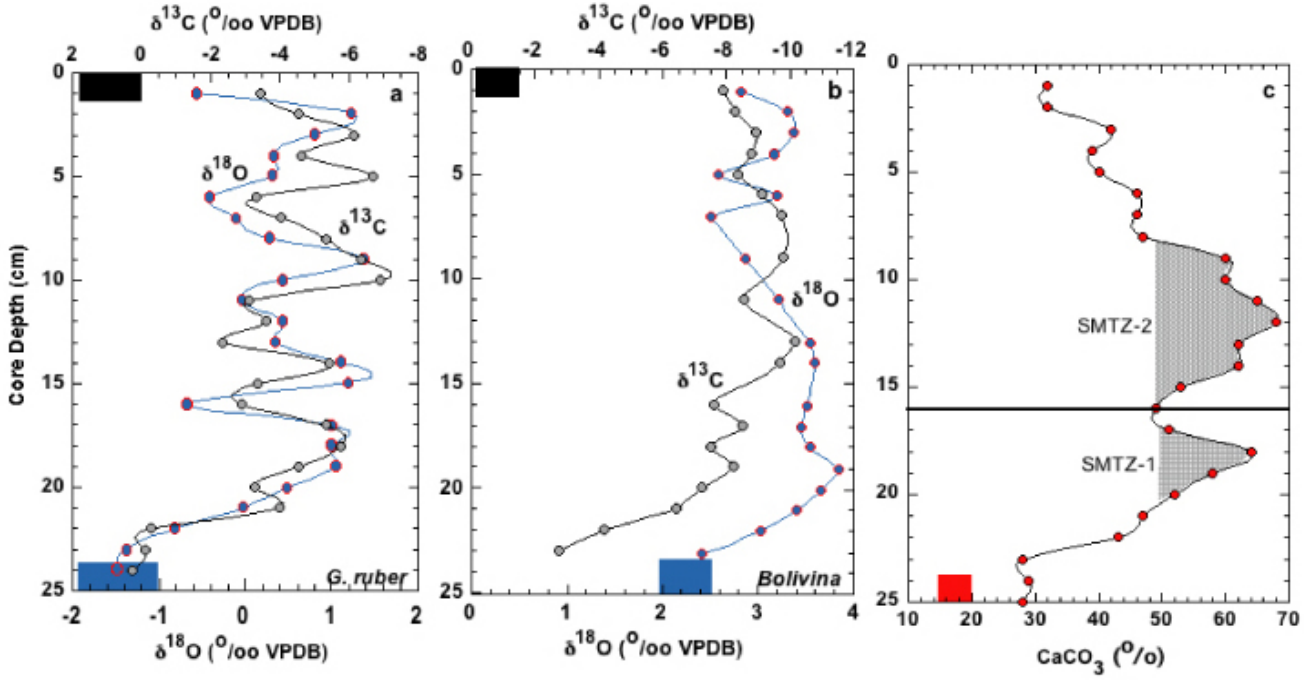

Fig. 11. Planktonic and benthic foraminiferal $\delta^{13}C$ and $\delta^{18}O$ profiles, and carbonate abundance graphed against core depths. Lines are drawn using cubic spline fits. (a) *G. ruber* profile. (b) *Bolivina* profile. Black and blue squares in (a) and (b) mark the $\delta^{13}C$ and $\delta^{18}O$ field of control samples, inclusive of uncertainties. (c) Abundance of carbonate nodules in percent. SMTZ-1 and SMTZ-2 mark the positions of two sequential sulfate-methane transition zones where anaerobic methane oxidation and carbonate precipitation reach maximum intensity and abundance. Red square represents carbonate abundance in hemipelagic sediments (9 ±2 cmKa^{-1}) from seep-free sites in the Gulf of Mexico (Santschi and Rowe, 2008).

of the SMTZ where anaerobic oxidation of methane (AOM) reaches the maximum activity (Panieri *et al.,* 2017). Of notice is the observation that the lower and higher sedimentation rates coincide with the peak carbonate abundances of SMTZ-1 and SMTZ-2, respectively (Fig. 11 c).

DISCUSSION

Cold-seep foraminifera

Our finding of multiple species of foraminifera (with tests stainable by Rose Bengal) living in sulfidic pore fluid under bacterial (*Beggiatoa*) mats, down to a sediment depth of about 5 cm, confirms previous results from the bathyal Gulf of Mexico (e.g., Sen Gupta and Aharon, 1994; Sen Gupta *et al.,* 1997). The dominant genus in this community is *Bolivina*. Numerous species of *Bolivina* and some other genera are known to tolerate, and even thrive, under severe dysoxia or microxia in diverse marine environments (Sen Gupta and Machain-Castillo, 1993; Bernhard and Sen Gupta, 1999). Studies at cold seeps and elsewhere demonstrate that some of them may even survive anoxia. This inference is supported by evidence beyond Rose-Bengal staining; Cell-tracker-green staining and ribosomal RNA analysis of diverse benthic foraminifers (raised in artificial benthic chambers) show that multiple genera and species can tolerate anoxia for many months (Langlet *et al.,* 2013). In several taxa (e.g., certain species of *Globobulimina, Nonionella, Stainforthia, Bolivina, and Uvigerina*), respiration under anoxia is linked to their capability of nitrogen storage and denitrification (e.g., Risgaard-Petersen *et al.,* 2006; Piña-Ochoa *et al.,* 2010; Orsi *et al.,* 2020). The common foraminifera of Green Canyon cold seeps are widely distributed in the bathyal zone of the northern Gulf of Mexico (Sen Gupta *et al.,* 2009); their particular strategy for survival or proliferation in an area of methane-hydrate dissociation is unclear.

Biostratigraphy

Of all the parameters of community composition, the most drastic stratigraphic change is observed in the density of total foraminiferal tests, expressed as number of tests in one gram of dry sediment. A rapid decline occurs in the oldest (24-19 cm) part of the core, i.e., between about 2.5 Ka and 2 Ka (Fig. 8 b). All values >2000 are confined to this lower section, whereas the values are mostly <100 in the younger samples, all the way to the core top. As explained earlier, the diversity changes are much more erratic, although reducing trends of species richness and Shannon Wiener Index are observed in the lowermost 5 cm of the core. We infer that hydrocarbon emissions began at our coring site more than 2500 years ago, reaching a high around 2 Ka, and continuing till the present day. The effect of this historical event had an impact on the foraminiferal community similar to that of the well-known 2010 Deepwater Horizon oil spill. That anthropogenic event, causing a large influx of polycyclic aromatic hydrocarbons in the benthic environment and "persistent reducing conditions"

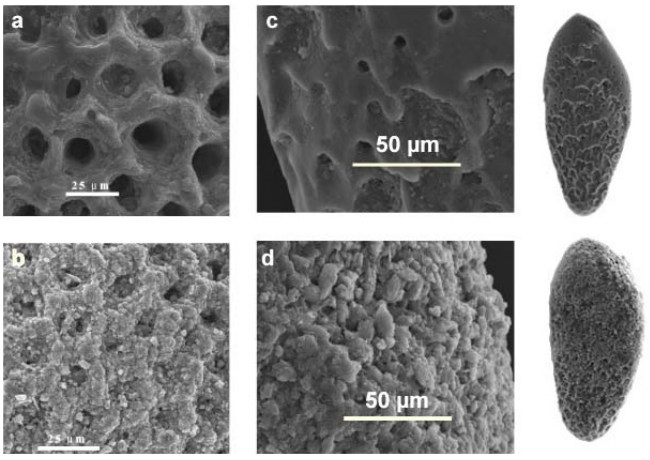

Fig. 12. Scanning Electron-Microscope (SEM) images of *G. ruber* and *Bolivina* tests from control and JSL-2900-PC2 cores. (a) Clean surface of a *G. ruber* test from a control site. (b) Secondary calcite overgrowths coating the test surface and filling the wall pores. (c) Smooth, clean wall of a well-preserved *Bolivina albatrossi* test from a control site; whole specimen to the right. (d) Heavily coated *Bolivina albatrossi* test with secondary calcite overgrowths; whole specimen to the right.

Table 2. Carbon and oxygen isotope compositions of paired planktonic and benthic foraminiferal calcite tests from core JSL-2900-PC2. The core was acquired at 567 m WD from a hydrate mound in GC-232 (Figs. 1 and 3), using the *Johnson-Sea-Link* II submersible. Planktonic, Gr=*Globigerinoides ruber*; benthic, Bol=single or mixed species of *Bolivina albatrossi* and *Bolivina ordinaria*. Isotope determinations at some core depths are missing because of the absence of *Bolivina* tests. CaCO3 (%) column marked "Carb" list the abundances of coarse and fine carbonate fractions (minus foraminiferal tests) and their isotope compositions. Control samples from core tops in hydrate-free sites at WD similar to our studied sediment core are listed at the bottom of the table.

Core Depth (cm)	$\delta^{13}C$ (Gr) (^{o}/oo VPDB)	$\delta^{18}O$ (Gr) (^{o}/oo VPDB)	$\delta^{13}C$ (Bol) (^{o}/oo VPDB)	$\delta^{18}O$ (Bol) (^{o}/oo VPDB)	$CaCO_3$ (%)
1	-3.4	-0.6	-7.9	2.8	32
2	-4.5	1.2	-8.3	3.3	32
3	-6.2	0.8	-8.9	3.4	42
4	-4.6	0.3	-8.8	3.2	39
5	-6.7	0.3	-8.4	2.6	40
6	-3.3	-0.4	-9.1	3.2	46
7	-4.0	-0.1	-9.7	2.5	46
8	-5.3	0.3			47
9	-6.4	1.4	-9.8	2.9	60
10	-6.9	0.4			60
11	-3.1	-0.1	-8.5	3.2	65
12	-3.6	0.4			68
13	-2.4	0.4	-10.2	3.5	62
14	-5.4	1.10	-9.7	3.6	62
15	-3.4	1.2			53
16	-2.9	-0.7	-7.6	3.5	49
17	-5.3	1.0	-8.5	3.5	51
18	-5.8	1.0	-7.5	3.5	64
19	-4.5	1.1	-8.2	3.9	58
20	-3.3	0.5	-7.2	3.7	52
21	-4.0	0.0	-6.4	3.4	47
22	-0.3	-0.8	-4.2	3.0	43
23	-0.1	-1.4	-2.7	2.4	28
24	0.3	-1.4			29
25					28
WD (m)					
564	1.1	-2.1	-1.7	3.0	
579	-0.2	-1.1	-2.1	2.0	
579	1.1	-1.0	-1.2	2.3	
549	0.6	-1.8	-1.6	1.6	
595	1.4	-1.3	-1.1	1.9	

(Schwing *et al.,* 2015), lowered both foraminiferal density and diversity in the surface sediment (~0–10 mm), but not to the same extent; the density decreased by 80-93%, but the species richness by only 30-40% (Schwing *et al.,* 2017; Schwing and Machain-Castillo, 2020).

Stable-Isotope Geochemistry

The stable-isotope geochemistry results are graphed in Figure 11. Planktonic and benthic foraminifera studied here are separated by a water column of about 560 m, and their primary biogenic calcite tests grow under vastly different water temperature and chemistry conditions, reflected in their distinctive isotope fields of control samples (Fig. 11). The question is why $\delta^{13}C$ and $\delta^{18}O$ values of the control planktonic and benthic calcite tests are markedly different (Table 2), as expected from their distinct habitats, yet exhibit comparable isotope anomalies once they are buried in the hydrate-bearing sediment.

Scanning Electron Microscope (SEM) images from control and hydrate mound sites offer clear evidence of foraminifera tests serving as templates for carbonate overgrowths (Fig. 12). These overgrowths are the product of gas-hydrate dissociation, where methane released in the pore fluids fuels a linked chain of biogeochemical processes.

Rapid exhaustion of dissolved oxygen by aerobic bacteria at the water-sediment interface promotes establishment of a consortium of methane-oxidizing archaea (methanotrophs) and sulfate-reducing bacteria (thiotrophs) that engage in coupled chemosynthesis at the SMTZ. This consortium uses methane derived from the gas hydrate dissociation as a source of reduced carbon and seawater-derived sulfate as a source of oxygen to gain energy required to perform metabolism from the reduction of sulfate to hydrogen sulfide (Aharon, 2000).

$$CH_4 + SO_4^{-2} \text{---> } H_2S + HCO_3^- + OH^- \quad (1)$$

$$Ca^{+2} + 2HCO_3^{-1} \text{---> } CaCO_3 + H_2O + CO_2 \quad (2)$$

The free-energy of reaction (1) is $\Delta Go = -17$ KJ mol^{-1} and therefore it is thermodynamically favorable to occur spontaneously (Alperin and Hoehler, 2009).

The biochemical reaction of coupled methane oxidation-sulfate reduction alters the seawater-derived pore-fluid chemistry as follows (Figs 5 b and 5 c): (i) depletion of sulfate; (ii) build-up of sulfide (iii) freshening of pore fluids accompanied by ^{18}O-enrichment; (iv) release of ^{13}C-depleted bicarbonate inherited from the methane oxidation process; (v) increased alkalinity and Dissolved Inorganic Carbon (DIC), and (vi) carbonate supersaturation, promoting deposition of authigenic carbonate in the form of nodules and overgrowths on foraminiferal templates (Fig. 11).

Additional observations emerging from a comparison of the downcore isotope profiles in Figure 11 have important bearings on the source of methane in the underlying gas hydrate, the pattern and longevity of methane transport, and the methane flow controls on the epigenetic alterations of foraminiferal tests.

We postulate that the primary hydrocarbon seepage at our GC-232 site is crude oil from deep reservoirs (Fig. 2) that is metabolized by microorganisms to methane. Several lines of evidence support this argument: (i) biodegraded crude oil patches are abundant in the lower half of the core (Fig. 5 a); (ii) methanogenic degradation of crude oil long-chain alkanes, either through syntrophic bacteria-archaea aggregate metabolism or non-syntrophic methanogens, has been substantiated in field and laboratory experiments (Jones *et al.,* 2008; Zhou *et al.,* 2021; Borrel, 2022), and (iii) a biogenic origin of the methane in shallow gas hydrates underlying the sediment explains its instability, breakup and subsequent dissociation at the local pressure and water temperature (Fig. 4).

The longevity of the methane seepage is established on the basis of the radiocarbon dates (Fig. 5 a), and the isotope profiles in Figure 11. With one significant exception, both *G. ruber* and *Bolivina* isotope profiles exhibit anomalous $\delta^{13}C$ and $\delta^{18}O$ values that are attributed primarily to the carbonate overgrowths on foraminiferal tests by comparison with the control samples (Figs. 12 b and 12 d). The singular exception is the 2 cm interval near the core bottom where the foraminifera tests show minimal alteration (Figs. 12 a and 12 c) and their isotope compositions are near identical to the controls (Table 2, Figs. 11 a and 11 b). Using the sedimentation rates established for our core (Fig. 5 a) we estimate a radiocarbon date of 2.5 Ka for the initiation of methane flow at our coring site.

With the exception of the core bottom, the $\delta^{13}C$ and $\delta^{18}O$ profiles of the planktonic and benthic foraminiferal species exhibit pronounced differences. First, the *G. ruber* isotope profile (Fig. 11 a) contains five prominent isotope excursions over a 2.5 Ka duration that are absent from the Bolivina record (Fig. 11 b). Second, *Bolivina* isotope profiles exhibit appreciably greater $\delta^{13}C$ and $\delta^{18}O$ anomalous values by comparison with the *G. ruber* profiles. We attribute these differences to the following factors (i) there are marked dissimilarities in the size of the test-wall pores between *G. ruber* and *Bolivina*, the former being larger by a factor of five relative to the latter, and likely serving as template for both fine and coarse overgrowths (Figs. 12 a and 12 c); (ii) there are substantial isotope differences between carbonate grain sizes (Hackworth, 2005), and (iii) the planktonic and benthic species, whose tests occur together in the sediment, live in very different habitats. In this study, all specimens of *G. ruber* were allochthonous and dead, whereas some individuals of *Bolivina* were autochthonous and alive.

Recent studies have indicated that some benthic foraminiferal genera, such as *Bolivina,* are thriving under anoxic conditions using ^{13}C-depleted organic carbon in the pore fluids as a carbon and energy source (Orsi *et al.,* 2020; Gomaa *et al.,* 2021). Other studies have proposed that association of some benthic foraminifera with ^{13}C-depleted methanotrophs maybe the primary cause of the highly negative $\delta^{13}C$ values in the foraminiferal calcite (Schmidt *et al.,* 2021). The stable-isotope data reported here cannot either support or negate the possibility of *Bolivina* living in anoxic sediments, because the secondary overgrowths conceal the primary biogenic calcite isotope compositions.

CONCLUSIONS

The methane-hydrate dissociation site supports a diverse assemblage of benthic foraminifera that consists almost

entirely of calcitic perforate species, and includes many facultative anaerobes. These taxa are not restricted to cold seeps, but are widely distributed in the bathyal zone in the northern Gulf of Mexico.

The foraminiferal record in core JSL-2900-PC2 shows a precipitous decline in assemblage density in the lowermost part of the core, beginning at or before 2.5 Ka, and culminating at the start of the first sulfate-methane transition zone (SMTZ-1, Fig. 11 c), at about 2 Ka. Such a consequence of seafloor methane emission is similar to the decimation of foraminiferal populations caused by the Deepwater Horizon oil spill of 2010. The persistently low foraminiferal density at our Green Canyon coring site is an evidence of continuous methane seepage here for at least the past 2000 years.

Investigation of the Green Canyon anoxic, hydrate-bearing, sediment using paired planktonic (*Globigerinoides ruber*) and endobenthic (*Bolivina albatrossi* and *B. ordinaria*) foraminiferal species proves advantageous in the quest to unravel the history of methane flow sourced in gas hydrates at the threshold of stability. With the singular exception of the core bottom where isotope values fall within the field of control samples, the foraminifera $\delta^{13}C$ and $\delta^{18}O$ profiles exhibit highly anomalous negative and positive excursions, respectively. The inverse correlation of the isotope profiles is attributed to the discharge of ^{13}C-depleted methane and ^{18}O-enriched freshwater transported in the sediment during methane-hydrate dissociation events. Carbonate abundance in the form of nodules exhibit two major peaks of 65% and 70%, representing the paleo-depths of SMTZs where upward transport of methane and downward diffusion of seawater-derived sulfate are consumed by AOM consortia. Carbonate supersaturation, coupled with authigenic carbonate deposition in the pore fluids, occurs at the SMTZs where AOM reaches the maximum activity.

Both planktonic and benthic foraminifera serve as templates for secondary overgrowths infilling the test pores that conceal the isotope values of the primary biogenic calcite. Under these circumstances, the stable-isotope signature cannot be used as evidence to prove or disprove an anaerobic adaptation of endobenthic foraminifera.

ACKNOWLEDGEMENTS

We thank the pilots of the submersible Johnson Sea-Link II (Harbor Branch Oceanographic Institute) and the captain and crew of the surface support vessel R/V Edwin Link for assistance with diving and coring. Drs. Baoshun Fu and Matthew Hackworth are thanked for assistance with sampling and analyses on board the ship and on terra firma laboratories. The final manuscript benefited from comments by Dr. Aninda Mazumdar of the National Institute of Oceanography, Goa, India. The senior author's study was supported by a grant from NOAA-Sea Grant (NA-86RG0073) and a Mineral Management Service (MMS), Gulf of Mexico OCS Region, contract 14-35-0001-30660-19946.

A NOTE OF REMEMBRANCE

It was our privilege to know Indra Bir Singh as a cherished friend and colleague. We were delighted by his company, and inspired by his scholarship. We will miss him.

REFERENCES

Aharon, P. 2000. Microbial processes and products fueled by hydrocarbons at submarine seeps. In: Microbial Sediments (Eds. Riding, R. E., Awramik, S. M.). Springer-Verlag Berlin: 270-281.

Aharon, P. 2003. Meltwater flooding events in the Gulf of Mexico revisited: Implications for rapid climate changes during the last deglaciation. Paleoceanography 18 (4): 10.1029/2002PA000840.

Aharon, P., and Fu, B. 1997. Pore fluid chemistry reveal processes occurring in hydrocarbon seeps from deepwater Gulf of Mexico. Gulf Coast Association of Geological Societies Transaction 47: 653.

Aharon, P., and Fu, B. 2000. Microbial sulfate reduction rates and sulfur and oxygen isotope fractionations at oil and gas seeps in deepwater Gulf of Mexico. Geochimica et Cosmochimica Acta 64 (2): 233-246.

Aharon, P., and Fu, B. 2003. Sulfur and oxygen isotopes of coeval sulfate-sulfide in pore fluids of cold seep sediments with sharp redox gradients. Chemical Geology 195: 201-218.

Aharon, P., and Hackworth, M. 2001. Anomalous carbon isotope fractionations in hydrate-bearing sediments from the Gulf of Mexico: Are bacteria to be blamed? EOS, American Geophysical Union Transactions 82 (47): F-174.

Aharon, P., Schwarcz, H. P., Roberts, H. H. 1997. Radiometric dating of submarine hydrocarbon seeps in the Gulf of Mexico. Geological Society of America Bulletin 109 (5): 568-579.

Aitken, C. M., Bennett, B., Huang, H., Brown, A., Bowler, B. F. J., Oldenburg, T., Erdmann, M., and Larter, S. R. 2008. Crude-oil biodegradation via methanogenesis in subsurface petroleum reservoirs. Nature 451: 176-181. 10.1038/nature06484

Alperin, M. J., and Hoehler, T. M. 2009. Anaerobic methane oxidation by archaea/sulfate reducing bacteria aggregates: 1. Thermodynamic and physical constraints. American Journal of Science.309: 869-957. 10.2475/10.2009.01

Bernhard, J. M. and Sen Gupta, B. K. 1999. Foraminifera of oxygen depleted environments, p. 201-216. In Modern Foraminifera (Ed. Sen Gupta, B. K.), Kluwer Academic Publishers, Dordrecht.

Bordoloi, S. 2007. Biogeochemical Processes Fueledd by Hydrocarbon Emissions in Modern and Ancient Marine Sediments: Examples from the Italian Apennines and the Gulf of Mexico. Unpublished PhD Dissertation, The University of Alabama: 213 pp.

Borrel, G. 2022. A microbe that uses crude oil to make methane. Nature 601: 196-197.

Brewer, P. G. 2006. Gas hydrates and global climate change. Annals of the New York Academy of Sciences, 912 (1): 195-199. 10.1111/j.1749-6632.2000.tb06773.x.

Cannariato, K. G. and Stott, L. D. 2004. Evidence against clathrate-derived methane release to Santa Barbara basin surface waters? Geochemistry Geophysics Geosystems 5 (5): 10.1029/2003GC000600.

Dickens, G. R., O'Neil, J. R., Rea, D. K., and Owen, R. M. 1995. Dissociation of oceanic methane hydrate as a cause of the carbon isotope excursion at the end of the Paleocene. Paleoceanography 10 (6): 965-971.

Fu, B. 1998. A Study of Pore Fluids and Barite Deposits from Hydrocarbon Seeps: Deepwater Gulf of Mexico. Unpublished PhD Dissertation, Louisiana State University: 275 pp.

Gooday, A. J. 2003. Benthic Foraminifera (Protista) as tools in deep-water palaeoceanography: Environmental influences on faunal characteristics. Advances in Marine Biology, 46: 1-90.

Gooday, A. J. 2019. *Deep-Sea Benthic Foraminifera,* p. 684-705. In Encyclopedia of Ocean Sciences Vol. 2, (Ed. Steel, John H.), Elsevier, London, 3rd edition, 10.1016/B978-0-12-409548-9.09071-0.

Hackworth, M. S. 2005. Carbonate Records of Submarine Hydrocarbon Venting: Northern Gulf of Mexico. Unpublished PhD Dissertation, Louisiana State University: 315 pp.

Hackworth M., and Aharon P. 1998. Effects of gas hydrates on the precipitation of carbonates in seep sediments, deepwater Gulf of Mexico. Geological Society of America Abstracts with Programs 30 (7): A-331-332.

Hackworth, M., and Aharon, P. 2000. Carbonates as recorders of gas hydrate dissociation in the Gulf of Mexico. Geological Society of America Abstracts with Programs 32 (7): A-101.

Herguera, J. C., Paull, C. K., Perez, E., Ussler III, W., and Peltzer, E. 2014. Limits to the sensitivity of living benthic foraminifera to pore water carbon isotope anomalies in methane vent environments. Paleoceanography 29: 10.1002/ 2013PA002457.

Hesse, R. 2003. Pore water anomalies of submarine gas-hydrate zones as tool to assess abundance and distribution in the surface: What have we learned in the past decade? Earth-Science Reviews, 61: 149-179.

Hesse, R., and Harrison, W. E. 1981. Gas hydrates (clathrates) causing pore-water freshening and oxygen isotope fractionation in deep-water sedimentary sections of terrigenous continental margins. Earth and Planetary Science Letters 55: 453-462.

Hill, T. M., Kennett, J. P., and Valentine, D. L. 2004. Isotopic evidence for the incorporation of methane-derived carbon into foraminifera from modern methane seeps, Hydrate Ridge, Northeast Pacific. Geochimica et Cosmochimica Acta 68 (22): 4619-4627.

Jones, D. M., Head, I. M., Gray, N. D., Adams, J. J., Rowan, A. K., Torres, M. E., Martin, R. A., Klinkhammer, G. P., and Nesbitt, E. A. 2010. Post depositional alteration of foraminifera shells in cold seep settings: New insights from flow-through time-resolved analyses of biogenic and inorganic seep carbonates. Earth and Planetary Science Letters. 299: 10-22.

Joshi, R. K., Mazumdar, A., Peketi, A., Ramamurty, P. B., Naik, B. G., Kocherla, M., Carvalho, M. A., Mahalakshmi, P., Dewangan, P., and Ramana, M. V. 2014. Gas hydrate destabilization and methane release events in the Krishna-Godavari basin, Bay of Bengal. Marine and Petroleum Geology 58: 476-489. 10.1016/j.marpetgeo.2014.08.013

Kennett, J. P., Cannariato, K. G., Hendy, I. L., and Behl, R. J. 2000. Carbon isotopic evidence for methane hydrate instability during Quaternary interstadials. Science 288: 128–133.

Kvenvolden, K. A. 1995. A review of the geochemistry of methane in natural gas hydrate. Organic Geochemistry 23 (11/12): 997-1008.

Langlet, D., Geslin, E., Baal, C., Metzger, E., Lejzerowicz, F., Riedel, B., Zuschin, M., Pawlowski, J., Stachowitsch, M. and F. J. Jorissen, F. J. 2013. Foraminiferal survival after long-term in situ experimentally induced anoxia. Biogeosciences, 10: 7463-7480.

Lobegeier, M. K. and Sen Gupta, B. K. 2008. Foraminifera of hydrocarbon seeps, Gulf of Mexico. Journal of Foraminiferal Research, 38: 92-116.

MacDonald, I.R., Sager, W.W., and Peccini, M.B. 2003. Gas hydrate and chemosynthetic biota in mounded bathymetry at mid-slope hydrocarbon seeps: Northern Gulf of Mexico. Marine Geology 198: 133-158.

Maekawa, T., and Imai, N. 2006. Hydrogen and oxygen isotope fractionation in water during gas hydrate formation. Annals of the New York Academy of Sciences, 912 (1): 452-459.10.1111/j.1749-6632.2000.tb06773.x

Maslin, M., Owen, M., Day, S., Long, D. 2004. Linking continental-slope failures and climate change: Testing the clathrate gun hypothesis. Geology 32 (1): 53-56.

McCorkle, D. C., Keigwin, L. D., Corliss, B. H., and Emerson, S. R. 1990. The influence of microhabitats on the carbon isotopic composition o f deep-sea benthic foraminifera. Paleoceanography 5: 161-185.

Orsi, W. D., Morard, R., Vuillemin, A., Eitel, M., Worheide, G., Milucka, J, and Kucera, M. 2020. Anaerobic metabolism of foraminifera thriving below the seafloor. ISME Journal. 14: 2580-3594. 10.1038/s41396-020-0708-1

Panieri, G., Camerlenghi, A., Conti, S., Pini, G. A. and Cacho, I. 2009. Methane seepages recorded in benthic foraminifera from Miocene seep carbonates, Northern Apennines (Italy). Palaeogeography, Palaeoclimatology, Palaeoecology 284: 271-282.

Panieri, G., James, R. H., Camerlenghi, A., Westbrook, G. K., Consolaro, C., Cacho, I., Cesari, V., and Sanches Cervera, C. 2014. Global and Planetary Change. 122: 151-160.

Panieri, G., Lepland, A., Whitehouse, M. J., Wirth, R., Raaness, M. P., James, R. H., Graves, C. A., Cremiere, A., and Schneider, A. 2017. Diagenetic Mg-calcite overgrowths on foraminifera tests in the vicinity of methane seeps. Earth and Planetary Science Letters 458: 203-212.

Piña-Ochoa, E., Høgslund, S., Geslin, E., Cedhagen, T., Revsbech, N. P., Nielsen, L. P., Schweizer, M., Jorissen, F., Rysgaard, S. and Risgaard-Petersen, N. 2010. Widespread occurrence of nitrate storage and denitrification among foraminifera and Gromiida. Proceedings of the National Academy of Sciences, 107: 1148-1153.

Platon, E. 2001. Benthic Foraminifera in Two Stressed Environments of the Northern Gulf of Mexico. Unpublished PhD Dissertation, Louisiana State University: 290 pp.

Rathburn, A. E., Perez, M. E., Martin, J. B., Day, S. A., Mahn, C., Gieskes, J., Ziebis, W., Williams, D., and Bahls, A. 2003. Relationships between the distribution and sable isotopic composition of living benthic foraminifera and cold methane seep biogeochemistry in Monterey Bay, California. Geochemistry Geophysics Geosystems 4 (12): 10.1029/2003GC000595.

Risgaard-Petersen, N., Langezaal, A. M., Høgslund, S., Schmid, M. C., Op den Camp, H. J. M., Derksen, J. W. M., Piña-Ochoa, E., Eriksson, S. P., Nielsen, L. P., Revsbech, N. P., Cedhagen, T. and van der Zwaan, G. J. 2006. Evidence for complete denitrification in a benthic foraminifer. Nature, 443: 93-96.

Rohling, E. J. and Cooke, S. 1999. Stable oxygen and carbon isotopes in foraminiferal carbonate shells, p. 239-258. In Modern Foraminifera (Ed. Sen Gupta, B. K.), Kluwer Academic Publishers, Dordrecht.

Ruppel, C. D., Shedd, W., Miller, N. C., Kluesner, J., Frye, M., and Hutchinson, D. 2022. US Atlantic margin gas hydrates. In: World Atlas of Submarine Gas Hydrates in Continental Margins (eds. Mienert, J. et al.). Springer Nature Switzerland AG: 287-302.

Santschi, P. H., and Rowe, G. T. 2008. Radiocarbon-derived sedimentation rates in the Gulf of Mexico. Deep-Sea Research II. 55: 2572-2576.

Schmidt, C., Geslin, E., Bernhard J. M., LeKieffre, C., Svenning, M. M., Roberge, H., Schweizer, M., and Panieri, G. 2021. Deposit feeding of a foraminifera from an Arctic methane seep site and possible association with a methanotroph revealed by transmission electron microscopy. Biogeosciences Discussions. 10.5194/bg-2021-284

Schwing, P. T. and Machain-Castillo, M. L. 2020. Impact and resilience of benthic foraminifera in the aftermath of the Deepwater Horizon and Ixtoc 1 oil spills, p. 374-387. In: Deep Oil Spills- Facts, Fate, and Effects (Eds. Murawski, S. A., Ainsworth, C. H., Gilbert, S., Hollander, D. J., Paris, C. B., Schlüter, M. and Wetzel, D. L.), Springer, Cham, Switzerland.

Schwing, P. T., O'Malley, B. J., Romero, I. C., Martinez-Colón, M., Hastings, D. W., Glabach, M. A., Hladky, E. M., Greco, A. and Hollander, D. J. 2017. Characterizing the variability of benthic foraminifera in the northeastern Gulf of Mexico following the Deepwater Horizon event (2010–2012). Environmental Science and Pollution Research, 24: 2754-2769.

Schwing, P. T., Romero, I. C., Brooks, G. R., Hastings, D. W., Larson, R. A. and Hollander, D. J. 2015. A decline in benthic foraminifera following the Deepwater Horizon Event in the northern Gulf of Mexico. PLOS One, 10: 1-22.

Sen Gupta, B. K. and Aharon, P. 1994. Benthic foraminifera of bathyal hydrocarbon vents of the Gulf of Mexico: Initial report on communities and stable isotopes. Geo-Marine Letters 14: 88-96.

Sen Gupta, B. K., Lobegeier, M. K. and Smith, L. E. 2009. Foraminiferal Communities of Bathyal and Abyssal Hydrocarbon Seeps, Northern Gulf of Mexico: A Taxonomic, Ecologic and Geologic Study. U.S. Department of the Interior, Minerals Management Service, Gulf of Mexico OCS Region, New Orleans, Louisiana, U.S.A., OCS Study MMS 2009-013, 385 p.

Sen Gupta, B. K. and Machain-Castillo, M. L. 1993. Benthic Foraminifera in oxygen-poor habitats. Marine Micropaleontology, 20: 83-201.

Sen Gupta, B. K., Platon, E., Bernhard, J. M. and Aharon, P. 1997. Foraminiferal colonization of hydrocarbon-seep bacterial mats and underlying sediment, Gulf of Mexico slope. Journal of Foraminiferal Research, 27 (4): 292-300.

Sen Gupta, B. K., Smith, L. E. and Machain-Castillo, M. L. 2009. Foraminifera of the Gulf of Mexico, p. 87–129. In Gulf of Mexico–

Origins, Waters, and Biota, v. 1, Biodiversity (Eds. Felder, D.L. and Camp, D. K.), Texas A&M University Press, College Station.

Stott, L. D., Bunn, T., Prokopenko, M., Mahn, C., Gieskes, J., and Bernhard, J. M. 2002. Does oxidation of methane leave an isotopic fingerprint in the geologic record? Geochemistry Geophysics Geosystems 3 (2): 10.1029/2001GC000196.

Torres, M. E., Mix, A. C., Kinports, K., Haley, B., Klinkhammer, G. P., McManus, J., and de Angelis, M. A. 2003. Is methane venting at the seafloor recorded by $\delta^{13}C$ of benthic foraminifera shells? Paleoceanography 18 (3): 10.1029/2002PA000824.

Torres, M. E., Martin, R. A., Klinkhammer, G. P., and Nesbitt, A. 2010. Post depositional alteration of foraminferal shells in cold seep settings: New insights from flow-through time-resolved analyses of biogenic and inorganic seep carbonates. Earth and Planetary Science Letters. 299:10-22.

Warren, A. and Bouchet, P. 1993. New records, species, genera, and a new family of gastropods from hydrothermal vents and hydrocarbon seeps. Zoologica Scripta 22: 1-90.

Wefer, G., Heinze, P-M, and Berger, W. H. 1994. Clues to ancient methane release. Nature 369: 282.

Wuebbles, D. J. and Hayhoe, K. 2002. Atmospheric methane and global change. Earth-Science Reviews, 57: 177-210.

Zhou, Z., Zhang, C-jing, Liu, P-fei, Fu, L., Laso-Perez, R., Yang, L., Bai, L-ping, Li, J., Yang, M., Lin, J-zhang, Wang, W-dong, Wegener, G., Li, M., and Cheng, L. 2021. Non-syntrophic methanogenic degradation by an archaeal species. Nature. 10.1038/s41586-021-04235-2.